

Seismic Behavior of Coupled Shear Wall with Variation of Opening Dimensions and Considering the Performance Level of Frame

Saba Sarlakchivaei¹, Hamid Saber²

¹Graduate student of Civil Engineering, Ale-Taha Institute of Higher Education, Tehran, Iran

²Assistant Professor, Department of civil engineering, university of eyvanekey, Semnan, Iran

Abstract –In recent years, Coupled Shear Wall system has been used in tall and medium buildings because it has advantages such as providing large spaces for creating various uses in floor and architectural considerations as doors, windows, and doorways. So this was brought into the attention of the designers. The lateral structural response is exactly dependent on the shear walls behavior; therefor these elements must response well under different loading situation. So this paper aims to study the effects of near and far fault earthquakes on the two series of mid-rise frame with the steel plate shear wall with the coupling system. In both series, the coupled shear wall will be evaluated by variation of opening dimensions, one in length of 1 and another in length of 2 meters and the width of once 0.6 and again 0.9 meters with the height ground floor of 2.8 and other floors of 3 meters regular in the plan. Firstly, structures were model in ETABS computer software. Then, the nonlinear static and time history analysis were carried out. Subsequently, the performance of walls was studied using two coupled near and two far fault records. Finally in the nonlinear time history analysis was measured relative displacement, absolute displacement of floor, base shear, and in story base shear. The results show that with the increased opening dimension, the measure relative and absolute displacements were increased, also with decrease opening dimension, the measure base shear and in story base shear decreased.

Keywords–Coupled Shear Wall, Variation of Opening Dimension, Nonlinear Static Analysis, Time History Analysis, Performance Levels

I- INTRODUCTION

The steel shear wall has been used in North America, Canada and Japan for the last four decades as a gravity loads and side loads resistant system. [1-2] Because it

has advantages such as providing large spaces for creating various uses in floor and architectural considerations as doors, windows, and doorways. So this was brought into the attention of the designers. [3] The coupled shear wall system as a resist system to lateral forces has high resistance, high lateral stiffness and energy dissipation capability. [4]

Despite the importance of the opening category and the need to study its effects on system behavior, despite numerous years of research by researchers in this field, few numerical or laboratory studies have yet been conducted on the presence of opening in steel shear walls. [5] Can be mentioned for example: the pulse characteristics of near-field earthquakes and detailed analysis such as nonlinear static analysis (Pushover) and dynamic time history analysis and performance levels analysis for order to better predict the seismic behavior of structures with coupled shear wall with Variation of Opening Dimension under near and far-field earthquakes from fault, to design more efficient structures. The following researches can be mentioned:

II-METHODOLOGY

In 1974, Pauli investigated the enhancement of coupled shear wall ductility using the new reinforcement method. In this method, an armature knot was inserted into the beam in diameter and tight wraps were wrapped around them to prevent buckling of the diagonal reinforcement. He showed that the proposed reinforcement method significantly increases the energy absorption capacity of the coupling beams and that these beams will have a more stable response at higher cycles, without decreasing in strength and stiffness. [3] In 1992, Roberts et al. investigated the effect of central circular opening

on the cyclic behavior of steel shear panels. They showed that the hardness and strength of the panels with opening can be conservatively estimated by applying a linear decrease coefficient to the hardness and resistance of the panel without opening. [5] In 1995, Koblat et al. investigated in vitro the coupled shear wall interface beam. They performed an analytical work on the 18-story building with shear walls by replacing HPFRCC concrete at critical points and duplicate beams. They showed that the use of this concrete increases the shear strength of the concrete and increases the structural ductility, as well as the simulation results, the structural behavior of the earthquake, and the improved plastic joints and cracking control. [6] In 2011, Fahnesto and Borlow investigated several frames with a 6-storey steel coupled shear wall. Also, 3-storey laboratory samples from the checked models were made 6-storey models.

In this study, the beam sections of the specimens had 100%, 200% and 400% plastic capacity of the floor beams. They showed that by increasing the modulus of the plastic cross-section of the graft beam compared to the beam, the base shear increased and also displacement in the lower floors increased. [1] In 2012, they also investigated that they were 6 and 12 behavior and mechanism of steel coupled shear wall. They referred to the relationship of the coupling degree (DC). In this study, 32 buildings story were modeled based on a 9 story building pattern and two types of 1.8 and 2.8 m bonding beams with 25% to 600% plastic floors sections. They showed that as the bond length increased, the coupling degree did not always increase. [1] Sabouri et al. (2012) investigated the effect of changing the size and location of rectangular openings on the hardness and toughness of hardened steel panels (with a series of horizontal and vertical sheets) without hardening. They showed that the rectangular opening position is not of much importance in the behavior of hardened steel panels, whereas in non-rigid models, the toughness and resistance of the panel varies drastically with the change of the opening position. [5] Gholikhani and Hatami in 2015 investigated the lateral behavior of cold rolled steel shear walls with cover of steel panel in finite element method. They analyzed shear wall panels using Abacus finite element software and developed a simple method for modeling the screws connecting cover sheets to frame that allow to simulate breakdown at the joints. [7] In 2017, Shaynfar et al. investigated the steel shear wall based on the performance-based plastic design method. They compared the proposed method of performance-based plastic design with the AISC seismic code guidelines for designing a 4-storey office building with a

steel shear wall as a lateral load-resistant system. [8] In 2018, Sharbatdar and Khosroabadi examined the adequacy of codes for the seismic design of steel panel shear walls with geometrical and physical variables. They first designed a steel sheet shear wall system in a high seismic zone for a 5-story building with accordance in AISC 05-341 seismic requirements, then to investigate the seismic behavior of the structure and to achieve hysteresis curves under periodic load. And the influence of geometrical and physical variables on its behavior, considering the effects of local instability (buckling) and nonlinearity of materials, designed the model of the wall specimen and similar specimens having different dimensions, sections, and states (with openings and hardenings) were modeled and analyzed in the Abacus finite element program. They showed that with the increasing number of floors, mode of the main breakdown of wall appears as a general buckling at the foot of the column, which is accompanied by a deterioration of strength and hardness [9].

In this paper, the effect of opening dimensions On changes in performance levels of regular steel structures in plan under pulse record of near and far basin species is investigated. To achieve a more accurate response were used from nonlinear analyzes such as static nonlinear (cover) analysis and dynamic time history analysis and the seismic behavior of these structures was investigated by obtaining amount of the displacement relative, absolute, floor shear and base shear.

2. Theoretical Foundations of Research

2-1 Nonlinear Static Analysis (Pushover)

Due to the development process of loading regulations and design on the performance of structures and non-responsiveness of linear analysis to ensure the design accuracy for estimating the actual structure response in earthquake there are two solutions:

1-Nonlinear static analysis method

2-Nonlinear dynamic analysis method

The nonlinear static method has an acceptable ability to estimate nonlinear structural behavior. This method can accurately determine the needle displacements. Detection of fracture mechanism to ensure that prevention of weak floor or column mechanism - strong beam does occur with this method. In this method there are constant gravitational loads and the lateral load gradually increases. Nonlinear static analysis consists of two parts:

1- Capacity curve

2- Combine the results of the capacity curve with the structural requirement for system response estimation [10].

The pushover curve continues until the target displacement. This displacement is called in the FEMA 356- and improvement instructions the target displacement and the demand displacement in the 40ATC [11].

2-1-1 Target Relocation in FEMA-356

Target displacement represents the maximum relative displacement a building may experience under an earthquake. There are different methods of determining target location that are FEMA-356 and the same optimization procedure. The advantage of the method introduced in FEMA 356 - the method introduced in 40ATC - is its ease of application. In this method, a nonlinear static analysis must first be performed and the base shear curve obtained against the lateral displacement of the control point (Pushover Curve). From the resulting pushover curve, by calculating a set of coefficients, the target displacement can be obtained.

According to FEMA-356 and the Target Relocation Improvement Instruction is equal to:

$$\delta_t = C_0 C_1 C_2 C_3 S_a \frac{T_e^2}{4\pi^2} g$$

In order to calculate the target displacement, one must first calculate the effective principal alternation time (Te) as follows.

$$T_e = T_i \times \sqrt{\frac{K_i}{K_e}}$$

Where T_i is the main periodicity of the building assuming linear behavior and based on FEMA-356 obtained from a dynamic elastic analysis in seconds, K_i is the elastic lateral stiffness and K_e is the effective lateral stiffness of building along the desired length. It is worth noting that the values of T_i , T_e , K_i and K_e are obtained from the two-line diagram of the structural capacity curve.

C_0 is the correction factor for the relation of the spectral displacement of a degree of freedom to the roof displacement (reference displacement) of a degree of freedom.

C_1 is the correction factor for converting the calculated displacements from the elastic linear response to the maximum expected non-elastic displacements of the structure.

C_2 is the correction factor to take the shape of the hysteresis curve and reduce the stiffness and deterioration of the structural members' resistance to maximum displacements. This coefficient takes into account the quality and quality of the structure and the desired performance level.

C_3 is the correction factor to consider the increase in displacements caused by the dynamic effects of $p-\Delta$. S_a is the spectral acceleration based on the main periodicity of the structure and g is the acceleration of gravity. [11-12-13]

2-2 Dynamic Time History Analysis

In the nonlinear dynamic analysis method, the structural response is calculated by considering the nonlinear behavior of the materials and the non-geometric behavior of the structures. The method assumes that the stiffness and attenuation matrix can be changed from one step to the next, but is constant over each time step and the model response under earthquake acceleration is calculated numerically and for each time step. Nonlinear dynamic analysis is the most accurate method used in structural analysis. The main purpose of this method according to Equation 3 is to solve the dynamic equilibrium differential equation of motion. Nonlinear dynamic analysis is performed by two general methods of direct integration and modal analysis.

$$Ku(t) + C\dot{u}(t) + M\ddot{u}(t) = r(t)$$

In the above relation K , C and M are the stiffness, damping and mass matrices, respectively and u , \dot{u} and \ddot{u} are the displacement, velocity and acceleration vector, respectively. $r(t)$ is the vector of external forces. [14]

3. Specifications of Distant and Near Fault Records

In order to perform dynamic time history analysis, 4 off-field records and 4 near-fault records according to Tables 1 and 2 with pulse effect (8 records in total) were used. The magnitude of the record is between 6.2 and 7.6 on the Richter scale obtained from the Peer site. [15] The criterion for near-fault records based on Mr. Baker's 2007 proposal is based on the following three criteria. [16]

1-The pulse index is greater than 0.85.

2-The pulse is formed in the early moments of the mapping speed.

3- PGA earthquake record exceeds 30 m / s.

The soil type of records was considered type 3 according to Iranian Code 2800. [15] Using the aforementioned records for dynamic analysis of temporal history, the seismic behavior of steel structures along the coupled shear wall was obtained by variation of opening dimension changes.

Table1: Seismic characteristics of far-fault record

No.	Record Year	Richter	Distance from Fault (km)	The Dominate Period (s)	Maximum Earth Speed (cm/s)
1	Chi-CHI CHY101-W, Taiwan, 20 September, 1999	7/6	11/14	1/29	70/64
2	Imperial Valley, H- E01240, 15 October, 1979	6/5	10/4	0/75	31/58
3	Loma Prieta, G03090, 18 October, 1989	6/9	14/4	0/92	39/03
4	Northridge, CNP196, 17 January, 1994	6/7	15/8	0/8	60/7

Table2: Seismic characteristics of near-fault record

No.	Record Year	Richter	Distance from Fault (km)	The Dominate Period (s)	Maximum Earth Speed (cm/s)
1	Nigata Japan, NIGH11, 2004	6/6	8/9	1/8	36/4
2	Kobe, Japan, Takatori, 1995	6/9	1/47	1/6	170

3	Northridge, 01,Jensen Filter Plant 1994	6/7	5/43	3/5	67
4	Morgan Hill, Coyote Lake Dam (SW Abut)	6/2	0/53	1	62

4. Frames Modeling in ETABS Software

Two 8-storey frame reference sheets with shear wall variations, one with 1 m length and one with 2 m length and 0.6 m once width and with the other 0.9 m (4 frames total) with ground floor height of 2.8 m and the other 3 m regular floors were included in the plan with a span of 5 m for all structures.

Structural uses were considered residential and the soil was according to Iranian Code 2800 [17], and the acceleration ratio of the design was considered to be a very high relative risk zone ($0.PGA = 0.35$) for all structures.

The specifications of the materials used in the structure are as shown in Table 3. Solid sections are used for column sections. As shown in Fig. 1 (a), section 18IPE3, which forms one of the first floor pillars of all the structures under consideration, has a depth of 180 mm and a width of 273 mm. IPE sections have also been used for beam sections. As shown in Fig. 1B, the 160IPE cross-section, which is one of the first floor beams of all the structures under study, has a height of 82 mm and a low width of 5 mm and a total height of 160 mm. Is other dimensions of beam and column sections are shown in Table 4. Thickness of shear wall dimensions in all classes for steel structures with coupled shear wall with opening dimensions of 0.6x1, 0.9x9 and 0.6x2 40W cross section, 40mm and for 45W cross section 0.9x2mm, 45mm, 45mm Was used.

As shown in Figure 2, linear and nonlinear modeling of the aforementioned structures was performed 3D in ETABS version 2015 software. Also, according to Fig. 3, the results of nonlinear analysis such as static nonlinear and dynamic time history analysis of one frame with D grid line were investigated.

Table 3: Specifications used in buildings

Concrete Materials				Steel Materials			
Mass per unit volume	M	245	Kg/m ³	Density	M	795	Kg/m ³
Weight	W	2400	Kg/m ³	Unit Weight	W	7800	Kg/m ³
Elasticity Modulus	Es	105 × 18 / 2	Kg f/c m ²	Elasticity Modulus	Es	106 × 06 / 0	Kg f/c m ²
Poisson Ratio	v	0/2	0/2	Poisson Ratio	v	0/3	
Concrete compressive strength	fc	210	Kg f/c m ²	Steel Yield Stress	fy	2400	Kg f/c m ²
Steel Yield Stress	fy	3000	Kg f/c m ²	Steel Ultimate Strength	fu	3600	Kg f/c m ²
Shear reinforcement Yield stress	fys	3000	Kg f/c m ²				

Beam Dimensions				
Floors	Beams around	Linked beams	Beams around	Beams around
1	IPE160	IPE100	IPE160	IPE600
2	IPE160	IPE100	IPE160	IPE600
3	IPE160	IPE100	IPE160	IPE600
4	IPE14F C1	IPE100	IPE160	IPE600
5	IPE600	IPE600	IPE600	IPE600
6	IPE600	IPE600	IPE600	IPE600
7	IPE600	IPE600	IPE600	IPE600
8	IPE600	IPE600	IPE600	IPE600

Table 4: Dimensions of steel structures with coupled shear wall with opening variations of 1x0.6, 1x0.9, 2x0.6 and 2x0.9

Column Dimensions					
Floors	Columns around	Coupled shear wall column	Coupled shear wall column	Columns around	Columns around
1	3IPE18	3IPE30F F2	3IPE30F F2	3IPE24	3IPE22
2	3IPE16F A1WA2	3IPE27F D2	3IPE30F A2WA1	3IPE27	3IPE22
3	3IPE18	3IPE22F B1WB2	3IPE27F A2	3IPE24	3IPE24
4	3IPE20	3IPE22	3IPE20	3IPE24	3IPE22
5	3IPE18	3IPE20	3IPE27	3IPE22	3IPE20F A1
6	3IPE18F A1	3IPE20F C1WC2	3IPE24	3IPE22F A1	3IPE22
7	2IPE220 - 2PL6x150	3IPE14	3IPE27	3IPE22	3IPE22
8	3IPE20	3IPE24F A1WA2	3IPE27	3IPE20F A1	3IPE22

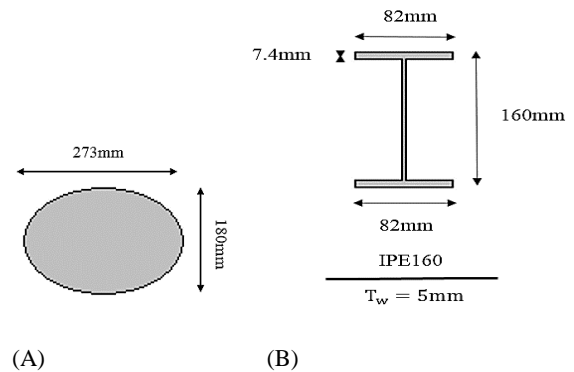


Figure 1: Sections of Steel Structures with Coupled Shear Wall with Opening Dimensions Changes in ETABS Software A) 3IPE18 B) IPE160

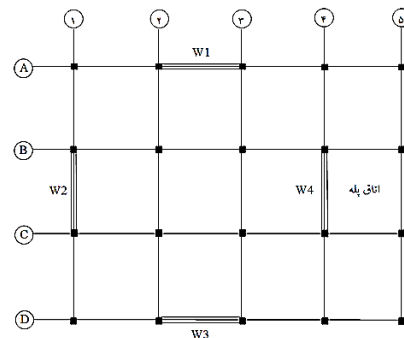
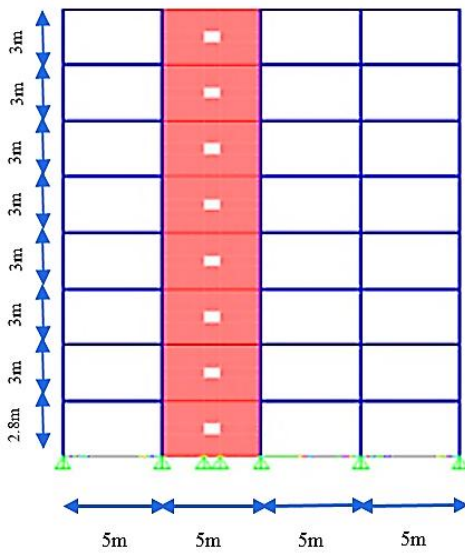
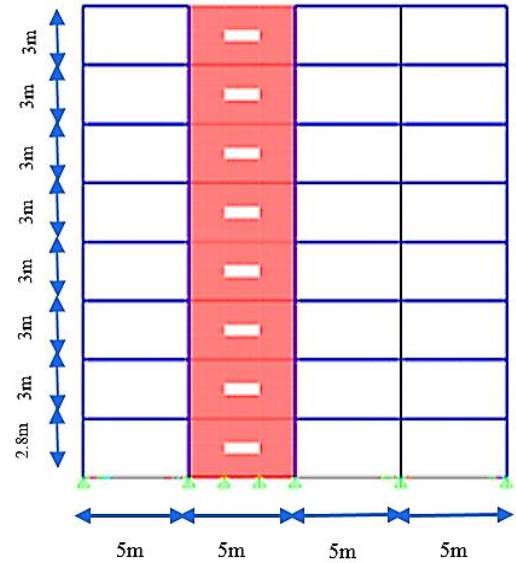


Figure 2: Buildings Plan

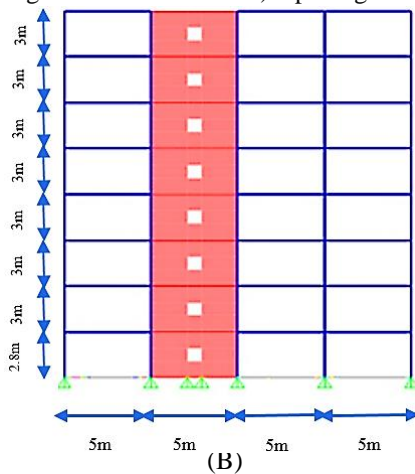


(A)

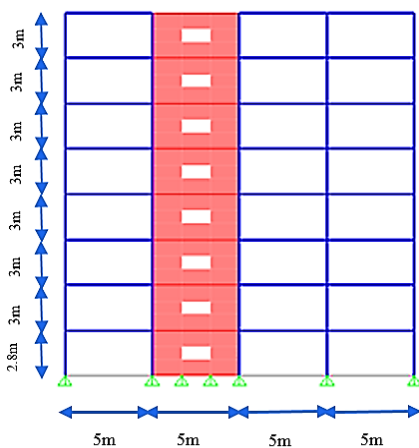


(D)

Figure 3: Steel Structures with Coupled Shear Wall with Opening Dimensions Changes for Nonlinear Analysis in ETABS Program with Grid Line D a) Opening Dimensions 1x0.9 b) Opening Dimensions 1x0.6 c) Opening Dimensions 2x0.9 d) Opening Dimensions



(B)



(C)

5. PERFORM ANALYSIS

5-1 Nonlinear Static Analysis

These structures were subjected to nonlinear static analysis in 3D. In this analysis, the lateral loading pattern of the first case and FEMA-356 constant coefficient method were used to determine the target displacement. By performing nonlinear static analysis for intermediate order structures with coupled shear wall system and obtaining displacement values in meters versus base shear in Kgf was drawn, to compare and evaluate the seismic performance, the 4-frame pushover curves with grid D are shown in a diagram as Figure 4.

The curves for the two design-basis earthquake hazard (DBE) and maximum considered earthquake (MCE) levels are two-line, with examples of these curves shown in Figure 5.

As shown in Fig. 4, with the slight increase in the cross-sectional area from 0.6 to 0.9 m², there is no differences were observed in their pushover curves but with the increase of the Opening area from 1.2 to 1.8 square meters, the pushover curve has gradually tilted downwards. By decreasing the cross section from 1.2 to 0.6 m² and also from 1.8 to 0.9 m², the ultimate resistance value decreased by 1.5 and 2.5%, respectively, this indicates that the effect of the area of the Opening under study on the seismic performance of the frame is very small.

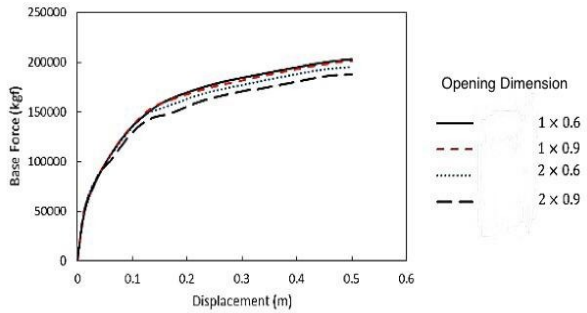


Figure 4: Comparison of Pushover curves

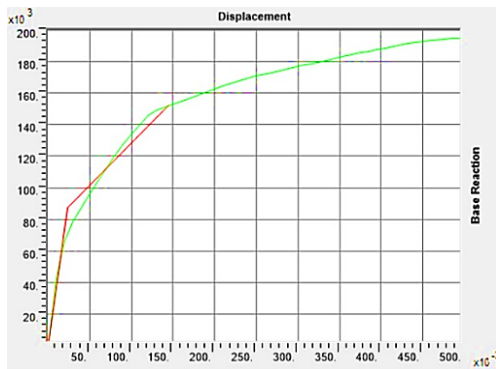


(D)

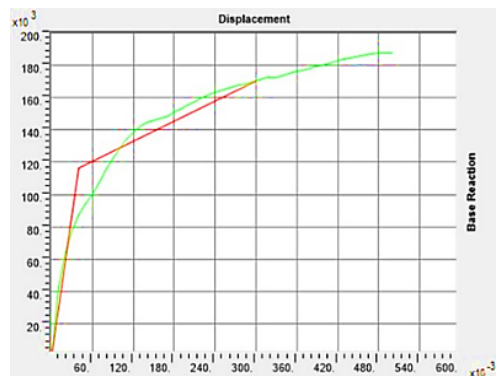
Figure 5: Dual Linearization of Pushover Curves in ETABS Software A) Opening Dimensions 2x0.6 at Maximum Considered Earthquake (MCE) b) Opening Dimensions 2x0.6 at Design Basis Earthquake (DBE) c) Opening Dimensions 2x0.9 at Maximum Considered Earthquake (MCE) c) Opening Dimensions of 2x0.9 at Design Basis Earthquake (DBE)



(A)



(B)



(C)

5-1-1 Control of Shear Wall Performance Levels

According to the Journal 360, shear wall permitted values for plastic rotation for life safety performance (LS) are 0.010 and the collapse prevention (CP) is 0.015.

The shear wall plastic rotation values were calculated for both design-basis earthquake (DBE) and maximum considered earthquake (MCE) and results are shown in Tables 5 and 6. As shown in Table 5, the plastic rotation values for all frames examined at hazard level of design basis earthquake are life safety performance and also, according to Table 6, the plastic rotation values for the very severe earthquake hazard level are equal the collapse prevention performance.

Table 5: Rotation shear wall plastic of samples at level of design-basis earthquake hazard for different floors

Earthquake hazard plan level	snoisnemiD gninepO 1×0/6			snoisnemiD gninepO 1×0/9			snoisnemiD gninepO 2×0/6			snoisnemiD gninepO 2×0/9		
stoolF	Displacement 1 (cm)	Displacement 2 (cm)	1 noitatoR citsalP	Displacement 1 (cm)	Displacement 2 (cm)	1 noitatoR citsalP	Displacement 1 (cm)	Displacement 2 (cm)	1 noitatoR citsalP	Displacement 1 (cm)	Displacement 2 (cm)	1 noitatoR citsalP
1	1/44	-0/69	0/004	1/42	-0/58	0/003	1/65	-0/55	0/004	1/66	-0/75	0/004
2	1/93	-0/78	0/005	1/92	-1/98	0/007	2/16	-0/76	0/005	2/1	-0/91	0/005
3	2/34	-0/95	0/005	2/35	-0/94	0/005	2/6	-0/92	0/006	2/47	-1/06	0/006
4	2/37	-1/06	0/006	2/54	-1/05	0/006	2/8	-1/04	0/006	2/63	-1/16	0/006
5	2/75	-1/14	0/006	2/77	-1/13	0/007	3/04	-1/13	0/007	2/82	-1/24	0/007
6	2/61	-1/18	0/006	2/84	-1/17	0/007	3/11	-1/17	0/007	2/87	-1/27	0/007
7	2/81	-1/19	0/007	2/84	-1/19	0/007	3/11	-1/18	0/007	2/87	-1/28	0/007
8	2/81	-1/2	0/007	2/84	-1/19	0/007	3/11	-1/19	0/007	2/87	-1/29	0/007

Table 6: Rotation shear wall plastic of samples at hazard level of design-basis extreme earthquake hazard for different floors

DBE Hazard level	snoisnemiD gninepO 1×0/6			snoisnemiD gninepO 1×0/9			snoisnemiD gninepO 2×0/6			snoisnemiD gninepO 2×0/9		
stoolF	Displacement 1 (cm)	Displacement 2 (cm)	1 noitatoR citsalP	Displacement 1 (cm)	Displacement 2 (cm)	1 noitatoR citsalP	Displacement 1 (cm)	Displacement 2 (cm)	1 noitatoR citsalP	Displacement 1 (cm)	Displacement 2 (cm)	1 noitatoR citsalP
1	4/5	-1/36	0/010	4/6	-1/32	0/010	4/78	-1/18	0/010	4/53	-1/58	0/010
2	5/14	-1/57	0/011	5/27	-1/52	0/011	5/4	-1/39	0/011	5/08	-1/63	0/011
3	5/68	-1/74	0/012	5/82	-1/7	0/013	5/9	-1/56	0/012	5/53	-1/79	0/012
4	5/91	-1/86	0/013	6/05	-1/82	0/013	6/12	-1/69	0/013	5/7	-1/9	0/013
5	6/18	-1/95	0/014	6/33	-1/9	0/014	6/38	-1/78	0/014	5/92	-1/98	0/013
6	6/24	-1/99	0/014	6/4	-1/95	0/014	6/45	-1/82	0/014	5/96	-2/02	0/013
7	6/24	-2	0/014	6/4	-1/96	0/014	6/45	-1/83	0/014	5/96	-2/03	0/013
8	6/24	-2/01	0/014	6/4	-1/97	0/014	6/45	-1/83	0/014	5/96	-2/03	0/013

5-2 Nonlinear Dynamic Analysis

Dynamic time history analysis for steel structures with coupled shear wall system with opening dimensional change in 3D was performed under distant and near fault records. The coupling acceleration of the selected mappings was scaled according to the following to Iranian Code . [17]

1. All mapping acceleration is scaled to its maximum value. This means that the maximum acceleration of them all equals the acceleration of gravity g .
2. The acceleration response spectrum of each pair of scaled acceleration mappings is determined by applying a damping ratio of 5%.
3. Response spectra of each coupled acceleration mapping using the combined square root method and make a single compound spectrum for each pair.
4. Hybrid response spectra of the three mapped acceleration pairs, averaged and compare the $T_2 / 0$ and $T_5 / 1$ alternation times with the standard design spectrum. Determine the scale coefficient such that the average values in any situation would not less than 1.4 times that of the standard range. T is the main periodic time of the building.
5. The specified scale factor shall be multiplied by the acceleration of the scaled mappings in paragraph 1 and used in dynamic analysis.

By performing dynamic time history analysis for structures listed under the acceleration of earthquake mapping Kobe – Japan as the nearest field obtained maximum values of relative displacement, absolute, floor shear and base shear that the frame with grid D the examples of the results are shown in Tables 7, 8 and 9 and Figures 6 and 7.

According to the tables and diagrams below, the relative and absolute displacements of the floors increase with increasing opening dimensions. Also, the shear rate of the floors and the base shear decreases with decreasing opening dimensions, indicating that opening dimensions has highly influence in seismic behavior of the coupled shear wall.

Table 7: Maximum relative displacement of floors with opening dimension changes

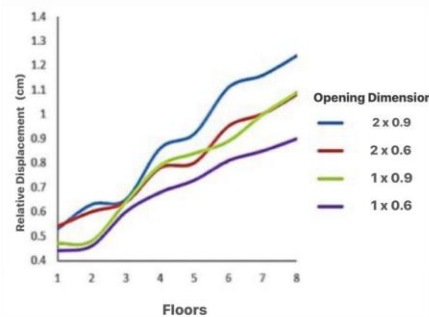
Maximum Relative Displacement (cm)	gninepO snoisnemiD 1×0/6	gninepO noisnemiD s 1×0/9	gninepO oisnemiD sn 2×0/6	gninepO isnemiD sno 2×0/9
Floor 1st	0/44	0/47	0/54	0/53
Floor 2nd	0/46	0/48	0/6	0/63
Floor 3rd	0/6	0/64	0/64	0/65
Floor 4th	0/68	0/79	0/78	0/86
Floor 5th	0/73	0/84	0/8	0/92
Floor 6th	0/81	0/89	0/95	1/11
Floor 7th	0/85	1	1	1/16
Floor 8th	0/9	1/09	1/08	1/24

Table 8: Maximum absolute displacement of floors with opening dimension changes

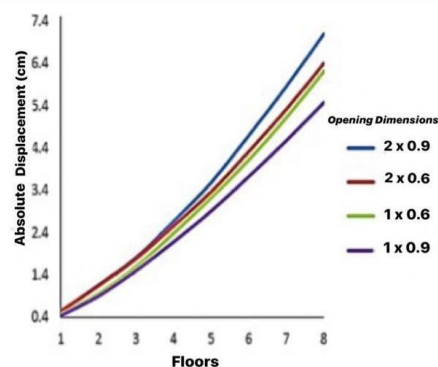
Maximum Absolute Displacement (cm)	gninepO snoisnemiD 1×0/6	gninepO noisnemiD s 1×0/9	gninepO snoisnemiD 2×0/6	gninepO g snemiD snoi 2×0/9
Floor 1st	0/44	0/47	0/54	0/53
Floor 2nd	0/9	0/95	1/14	1/16
Floor 3rd	1/5	1/59	1/78	1/81
Floor 4th	2/18	2/38	2/56	2/67
Floor 5th	2/91	3/22	3/36	3/59
Floor 6th	3/72	4/11	4/31	4/7
Floor 7th	4/57	5/11	5/31	5/86
Floor 8th	5/47	6/2	6/39	7/1

Table 9: Shear on floors with opening dimensions changes

Shear on Floors (t)	gninepO noisnemid 1×0/6	gninepO noisnemid 1×0/9	gninepO noisnemid 2×0/6	gninepO noisnemid 2×0/9
Floor 1st	124	138	148	171
Floor 2nd	118	128	135	156
Floor 3rd	108	120	127	141
Floor 4th	95	110	119	139
Floor 5th	88	96	110	130
Floor 6th	73	89	101	121
Floor 7th	65	77	93	110
Floor 8th	49	65	83	98

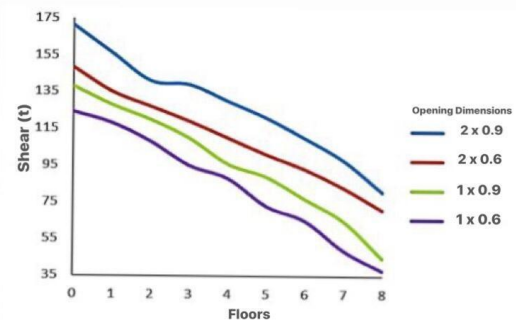


(A)



(B)

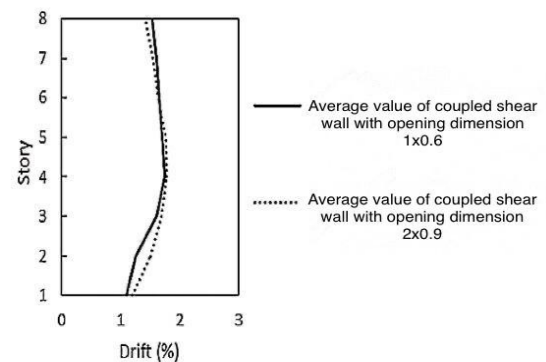
Figure 6: Comparison of displacement floors with opening dimensions changes a) Relative displacement b) Absolute displacement



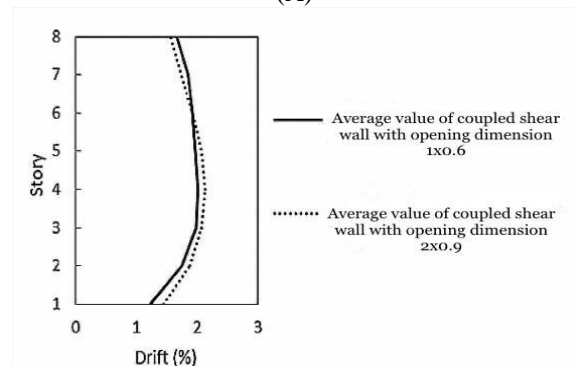
Figure

7: Comparison of shear on floors with opening dimension changes

In order to compare the seismic performance of the frames, the maximum mean values of displacement were calculated based on near and far fault records, an example of curve which is shown in Fig. 8. As shown in the figure below, Maximum values of midrange structural displacement with opening dimensions of 2x0.9 in relation to structures with opening dimensions of 1x0.6 under both far and near fault sets on the lower and middle floors are about 2% higher, indicating that the impacts it was not so noticeable.



(A)



(B)

Figure 8: Comparison of maximum measure of displacement between frame with coupled shear wall with opening dimensions of 1x0.6 and 2x0.9 a) In far-fault records b) In near-fault records

CONCLUSION

The results of the analysis of intermediate steel structures with the coupled shear wall system with considering changes of opening dimensions showed that:

- The relative and absolute displacements of the floors increase with the increase in the opening dimensions. Also, the amount of shear on the floors and the base shear is reduced by decreasing the opening dimensions, which indicates the large effect of the opening dimensions on the seismic behavior of the coupled shear wall with considering the performance levels of the frame.
- The performance level of all frames was within the design earthquake hazard level, in the area of lifesafety and in the extreme earthquake hazard level, in the collapse prevention.
- By increasing the opening dimensions, the stress around them as well as the wall foot is about 2% higher at similar performance levels. In addition, as the opening dimensions increase, the maximum stress extends to the upper floors relative to the walls of the smaller ones.
- The average maximum displacement of the frames under the near-fault records is about 25% higher than the far-fault records.
- The maximum displacement of the frame with the dimensions of 2x0.9 under the near and far records was 2% more than that of the frame with dimensions of 1x0.6. Therefore, the effect of increasing the assumed opening on the seismic performance of the frames is negligible and can be ignored.
- By increasing the opening dimensions from 1x0.6 to 1x0.9 in the shear wall, the ultimate strength does not change to some extent but with the further increase in the opening dimensions, the ultimate strength of the frames has finally been reduced to 2.5%.

REFERENCES

- [1] Gholhaki, Majid and Ghadkesar, Muhammad Bagher. (2018). Evaluation the performance of link beam length under nonlinear dynamic analysis in the coupled steel shear wall system with rigid joint. *Journal of Ferdosi Civil Engineering*, Vol. 30, No. 2, page (19-32).
- [2] Poursha, M. Khoshnoudian, F. and Moghadam, A.S. (2009). A consecutive modal pushover procedure for estimating the seismic demands of tall buildings. *Journal of Engineering Structures*, Vol. 31, page (591-599).
- [3] Razaz, Seyyed Mostafa. and Shariatmadar, Hashem. (2016). Evaluation the behavior of the coupled shear wall under the effect of near-fault earthquakes. *Journal of Ferdosi Civil Engineering*, Vol. 27, No. 1, page (1-16).
- [4] Rahgozar, Reza. Saffari, Hamed and Khani, Ahmad Sadegh. (2003). Determination of parametric stress distribution functions for approximation stress in the coupled shear wall. *The First Conference on Immunization and Structures Rehabilitation*, City: Tehran, Vol. 1.
- [5] Barkhordari, Mohammad Ali. Hossein Zadeh, Seyyed Ali Asghar and Sedighi, Mahdi. (2017). Evaluation of the behavior of steel shear walls with strengthen opening. *Journal of Sharif Civil*, Vol. 2/32, No. 1/2, page (79-89).
- [6] Sharbatdari, Mohammad Kazem. Shayani, Ehsan. and Khairuddin, Ali. (2019) Laboratory evaluation of the behavior of the coupled shear wall using the reinforced fiber concrete HPFRCC in link beam with different reinforcement arrangement. *Journal of Sharif Civil*, Vol. 2/34, No. 2/2, page (3-13).
- [7] Gholikhani, Morteza and Hatami, Shahabeddin. (2016). Lateral behavior of the cold-rolled steel shear walls with steel plate cover using finite element method *Journal of Modeling in Engineering*, Vol. 13, No. 40, page (129-150).
- [8] Shayanfar, Mohsen Ali. Raissi Dehkordi, Morteza, Rezaian, Alireza and Gohar Rokhi, Ali. (2018) Evaluation of steel shear wall based on plastic design based on performance. *Journal of Modeling in Engineering*. Vol. 15, No. 51, page (40-40).
- [9] Sharbatdar, Mohammad Kazem. Khosrowabadi, Mohammad. (2019). Evaluation the adequacy of codes for seismic design of shear walls with steel plate with geometric and physical variables *Journal of Modeling in Engineering*, Vol. 16, No. 52, page (24-24).
- [10] Tabesh pour, Mohammad Reza. (2018) Nonlinear analysis of structures. Edition 3. City Published: Fadak Isatis- Iran. page (1-340).
- [11] Taghinezhad, Ramin, (2017) Seismic design and rehabilitation of structures based on performance level with SAP2000 and ETABSE pushover analysis. Edition 5. City Published: Academic Books- Iran. page (1-388).
- [12] (2006) Seismic Design Code for Buildings. Ministry of Interior: Taipei, Taiwan.
- [13] Xinzheng, Lu. Xiao, Lu. Guan, H. Zhang, W. and Lieping, Ye. (2013). Earthquake-induced collapse simulation of a super-tall mega-braced frame-core tube building. *Journal of Constructional Steel Research*. Vol. 82, page (59-71).
- [14] Yeganeh Keyvani, Forough. Tahghighi, Hossien and Roshanai, Ahmad (2017) Seismic analysis of wicker cable bridges using dynamic time history and nonlinear static methods. 9th National Civil Engineering Congress.
- [15] Next Generation Attenuation of Ground Motions (Nga) Project (2006). <http://Peer.Berkeley.Edu/nga/> (Accessed 10 October 2006).
- [16] Baker, J.W. (2007). Plots of Identified Velocity Pulses. Department of Civil and Environmental Engineering. Stanford University, Stanford, CA 94305, USA.
- [17] J (2015). Code for designing buildings against earthquake-Standard 2800-05. Edition 20. City Published: Building and Housing Research Centre.